The Astrophysical Journal, 763:140 (11pp), 2013 February 1 doi:10.1088/0004-637X/763/2/140

THE ABUNDANCE OF PRESOLAR GRAINS IN COMET 81P/WILD 2

Christine Floss[1], Frank J. Stadermann[1], Anton T. Kearsley[2], Mark J. Burchell[3], and W. J. Ong[1]
[1] Laboratory for Space Sciences, Physics Department, Washington University, 1 Brookings Drive, St. Louis, MO 63130, USA; floss@wustl.edu
[2] Impacts and Astromaterials Research Centre, Science Facilities, Natural History Museum, London SW7 5BD, UK
[3] Centre for Astrophysics and Planetary Sciences, School of Physical Sciences, University of Kent, Canterbury, Kent CT2 7NH, UK
Received 2012 October 5; accepted 2012 December 6; published 2013 January 17

ABSTRACT

We carried out hypervelocity impact experiments in order to test the possibility that presolar grains are preferentially destroyed during impact of the comet 81P/Wild 2 samples into the *Stardust* Al foil collectors. Powdered samples of the ungrouped carbonaceous chondrite Acfer 094 were shot at 6 km s^{-1} into *Stardust* flight spare Al foil. Craters from the Acfer 094 test shots, as well as ones from the actual *Stardust* cometary foils, were analyzed by NanoSIMS ion imaging to search for presolar grains. We found two O-rich presolar grains and two presolar SiC grains in the Acfer 94 test shots, with measured abundances in the foils of 4 and 5 ppm, respectively, significantly lower than the amount of presolar grains actually present in this meteorite. Based on known abundances of these phases in Acfer 094, we estimate a loss of over 90% of the O-rich presolar grains; the fraction of SiC lost is lower, reflecting its higher resistance to destruction. In the *Stardust* cometary foils, we identified four O-rich presolar grains in 5000 μm^2 of crater residue. Including a presolar silicate grain found by Leitner et al., the overall measured abundance of O-rich presolar grains in Wild 2 is ∼35 ppm. No presolar SiC has been found in the foil searches, although one was identified in the aerogel samples. Based on the known abundances of presolar silicates and oxides in Acfer 094, we can calculate the pre-impact abundances of these grains in the *Stardust* samples. Our calculations indicate initial abundances of 600–830 ppm for O-rich presolar grains. Assuming a typical diameter of ∼300 nm for SiC suggests a presolar SiC abundance of ∼45 ppm. Analyses of the *Stardust* samples indicated early on that recognizable presolar components were not particularly abundant, an observation that was contrary to expectations that the cometary material would, like interplanetary dust particles, be dominated by primitive materials from the early solar system (including abundant presolar grains), which had remained essentially unaltered over solar system history in the cold environment of the Kuiper Belt. Our work shows that comet Wild 2, in fact, does contain more presolar grains than measurements on the *Stardust* samples suggest, with abundances similar to those observed in primitive IDPs.

Key words: astrochemistry – circumstellar matter – comets: individual (81P/Wild 2) – Kuiper Belt: general

Online-only material: color figures

1. INTRODUCTION

The study of presolar grains ("stardust') in the laboratory has been an active field of extraterrestrial materials research for more than 20 years (e.g., Zinner 2007). These grains condensed in stellar environments before being embedded in a variety of host phases during the formation of the solar system. Presolar grains that escaped destructive parent body processes, such as thermal metamorphism and aqueous alteration, can today be found at low abundances in relatively unaltered extraterrestrial materials including interplanetary dust particles (IDPs), primitive meteorites, Antarctic micrometeorites, and cometary matter (Lewis et al. 1987; Tang & Anders 1988; Amari et al. 1990; Messenger et al. 2003a; McKeegan et al. 2006; Nguyen & Zinner 2004; Yada et al. 2008). Much of the research on presolar grains has focused on determining their stellar origins and history through isotopic, elemental, and structural studies in an effort to better constrain fundamental astrophysical processes, such as stellar nucleosynthesis, condensation parameters, interstellar processing, and galactic chemical evolution (e.g., Nittler 2005; Bernatowicz et al. 2006; Meyer & Zinner 2006; Gyngard et al. 2009).

However, it is also possible to make use of the very presence or relative abundance of presolar grains in various types of host materials to learn about different degrees of pre-accretionary alteration or parent body processing throughout solar system history. The abundance of presolar grains in a given type of extraterrestrial material thus becomes a measure of how well the host material has preserved the original starting material from the solar nebula (Huss 1990, 1997, 2004; Huss & Lewis 1995; Huss et al. 2003, 2006; Floss & Stadermann 2009, 2012; Trigo-Rodríguez & Blum 2009). The inferred degree of primitiveness can be used as a first-order hierarchical ranking of different types of solar system materials, from completely differentiated samples, which no longer contain any recognizable presolar components, to the most unaltered materials, whose compositions—among those studied in the laboratory—come closest to that of the mix of primordial and newly condensed materials in the protoplanetary disk. This ranking scheme has been studied in detail for meteorites of different groups and petrologic types, but has also been extended to other types of extraterrestrial materials, such as select groups of IDPs and Antarctic micrometeorites, some of which have higher abundances of presolar grains and are therefore considered "more primitive" than the least-metamorphosed chondritic meteorites (Messenger et al. 2003a; Floss et al. 2006; Yada et al. 2008; Busemann et al. 2009). In this context, the abundance of presolar grains in cometary material became one of the key questions when NASA's *Stardust* mission returned samples from comet 81P/Wild 2 for laboratory investigation (Brownlee et al. 2006, 2009).

While the determination of presolar grain abundances in meteoritic samples is fairly straightforward and can be accomplished with a standardized analytical approach (e.g., Floss &

Stadermann 2009; Vollmer et al. 2009; Nguyen et al. 2010), the same is not true for cometary samples from the *Stardust* collector. Difficulties with the *Stardust* samples include: the small size of the individual samples (e.g., dust grains), the physical effects of their collection at 6.1 km s^{-1} via impacts onto Al foil and into aerogel, and the problems associated with efficiently extracting material for analysis from the resulting craters and tracks.

Notwithstanding these difficulties, analyses indicated early on that recognizable presolar components were not particularly abundant in the returned samples. In fact, during the nine months of the coordinated initial survey of the cometary samples (the preliminary examination or PE), only a single presolar grain was positively identified (McKeegan et al. 2006; Stadermann et al. 2008). This observation went contrary to some earlier expectations (see below) and, together with the discovery of a significant portion of high-temperature minerals among the cometary materials, represented one of the biggest surprises of the *Stardust* cometary sample PE (A'Hearn 2006; Brownlee et al. 2006; McKeegan et al. 2006; Zolensky et al. 2006). Several additional presolar grains have since been identified in material from comet 81P/Wild 2 (Stadermann & Floss 2008; Messenger et al. 2009; Leitner et al. 2010). In this paper, we discuss the observational evidence from the *Stardust* foil analyses in detail and demonstrate how laboratory test shots of meteoritic material can be used to investigate preservation bias and thereby help to calibrate the absolute presolar grain abundances in matter from comet 81P/Wild 2. Some aspects of this work have previously been reported (Stadermann & Floss 2008; Stadermann et al. 2009a, 2009b).

2. SAMPLES AND EXPERIMENTAL METHODS

2.1. Comet 81P/Wild 2

Comet 81P/Wild 2 was discovered in 1978 (Wild 1978) and was subsequently observed during perihelion passages in 1984, 1990, 1997, 2003, and 2010 (Farnham & Schleicher 2005; Królikowska & Szutowicz 2006; Farnham et al. 2010). NASA's *Stardust* mission was launched in 1999 February, encountered comet 81P/Wild 2 in 2004 January, and successfully returned samples to Earth in 2006 January (Brownlee et al. 2003, 2004, 2006). During the cometary flyby, the spacecraft was bombarded by coma dust particles with impact speeds of 6.12 km s^{-1}; this dust was collected on the exposed cometary collector surface, which consisted of 1039 cm^2 of silica aerogel and 153 cm^2 of Al 1100 foil (Tsou et al. 2003).

Cometary dust grains impacting the aerogel collector produce tracks in the low-density, highly porous material (see Burchell et al. 2006 for a discussion of the use of silica aerogel as a dust collector in space). Matter from the impactor can be found as fragments and solidified melt along the track walls or as terminal particles at the ends of the tracks. Peak shock pressures in the aerogel collectors have been estimated to be on the order of 800 MPa and tracks can be millimeters in length, indicating a relatively gentle deceleration during capture (Trigo-Rodríguez et al. 2008). Nevertheless, work on the aerogel tracks has shown that these conditions are sufficient to easily disrupt and break apart cometary dust grains, unless they are well consolidated and robust (Burchell et al. 2008; Kearsley et al. 2012). The excellent thermal insulation properties of the aerogel, its composition, and fine porous structure combine to promote high-temperature mixing of the impactor material with the aerogel. Unless bound into more robust coarse grains, all fine-grained ($<\mu$m scale) cometary material collected in *Stardust* aerogel is, therefore, likely to have undergone extensive processing and mixing. The gross morphology of the *Stardust* tracks does not itself provide an unambiguous indication of impacts by particles dominated by fine-grained, porous aggregate material, as the experimental evidence of Kearsley et al. (2012) shows that similar bulbous track shapes can be created by aggregates of either very fine or rather coarser ($>\mu$m), crystalline aggregates. However, Leroux (2012) has now shown that widely dispersed melt on the surface of some bulbous *Stardust* tracks carries elemental ratios close to the chondritic CI composition, which probably reflects an origin in very fine-grained material like that seen in chondritic porous IDPs. We might expect this fine-grained material from Wild 2 to be accompanied by substantial numbers of presolar grains. Unfortunately, the aerogel tracks present very large, irregular, and rather inaccessible surface areas, which require complex preparation before the material is suitable for analysis.

In contrast, the impacts onto the Al foils created distinctive craters, whose sizes and shapes have been extensively described (Hörz et al. 2006; Kearsley et al. 2006; Price et al. 2010). It has been estimated that peak shock pressures during impacts into the foils were in the range of 55–90 GPa (Burchell & Kearsley 2009), significantly higher than the pressures in the aerogel tiles. However, post-shock temperatures were almost certainly quenched by the excellent thermal conductivity of the cold metal foil. Studies (e.g., Leroux et al. 2008; Wozniakiewicz et al. 2012a) have noted the presence of extensive projectile residue retained within the craters. Moreover, the foils require relatively little sample preparation prior to analysis and, therefore, provide a much more straightforward substrate for determining the abundance of presolar grain in these samples, although a detailed understanding of impactor preservation bias (due to shock processing) is essential.

Since the return of these cometary samples, we have carried out NanoSIMS measurements on a variety of samples from Wild 2, including transmission electron microscopy (TEM) sections of cometary particles embedded in aerogel, aggregates of grains extracted from aerogel and pressed into high-purity Au, and residues present in impact craters on the Al foils. As the foils provide projectile residue that is easily accessible for NanoSIMS measurements, the bulk of our measurements have focused on craters. Table 1 summarizes the craters we have analyzed to date. These include a 72 μm crater from foil C2118N, a 28 μm crater from C2116N, and 20 craters of various sizes from foil C2010W. In addition, foil C2086W contains a large (295 μm) crater that completely penetrated the Al foil (e.g., Kearsley et al. 2008); the residue from this crater contains the first presolar grain identified from Wild 2 material (McKeegan et al. 2006; Stadermann et al. 2008).

2.2. Acfer 094 Test Shots

To test the efficiency of presolar grain capture, preservation, recognition, and measurement in *Stardust* foil craters, and hence to understand possible biases in the results of the *Stardust* measurements, we designed an experiment with a well-characterized control sample. The Acfer 094 ungrouped carbonaceous chondrite is known to contain abundant presolar grains (Bland et al. 2007; Nguyen et al. 2007; Vollmer et al. 2009). A small ($\sim$10 mm^3) sample of this meteorite was ground in a small agate mortar and sieved to exclude surviving large grains ($>53\ \mu$m). Two sub-samples of the powder (labeled 1a and 2a; Table 1) were fired as buckshot (i.e., many grains per shot) at *Stardust* flight spare Al 1100 foil (Figure 1) with the

Table 1
Foils and Craters Analyzed for Presolar Grain Searches

Foil[a]	No. of Craters	Diameter(s) (μm)	Measured Area (μm^2)	Presolar Grains
Stardust Wild 2				
C2086W[b]	1	295	1330	1 O-rich
C2118N	1	72	2335	1 O-rich
C2116N	1	28	1000	1 O-rich
C2010W	20	0.5–7.5	330	1 O-rich
Total			4995	
Test Shots				
Acfer 094 1a	43	1.5–90	10685	1 SiC
Acfer 094 2a	20	4.0–58	6430	2 O-rich
Acfer 094 3a	25	6.4–59	7670	1 SiC
Total			24785	
Stardust Wild 2[c]				
C2013N, C2037N, C2044W, C2052N, C2086N, C2126W	236	0.24–1.76	86	1 O-rich

Notes.
[a] The naming convention for the foils refers to their location on the collector (see Kearsley et al. 2006 for details)
[b] Data from McKeegan et al. (2006) and Stadermann et al. (2008).
[c] Data from Leitner et al. (2012).

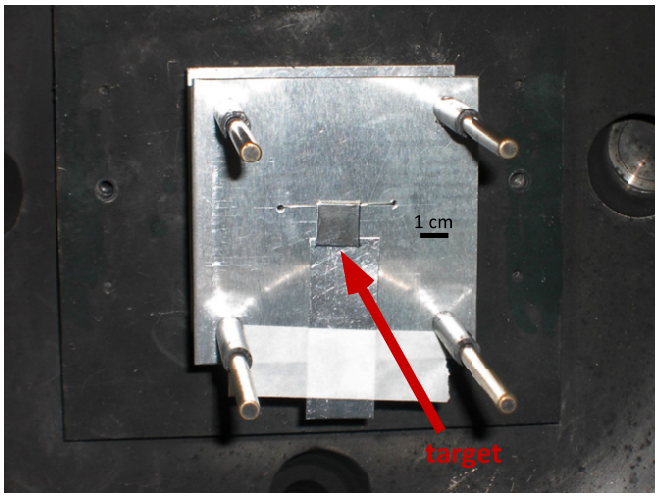

Figure 1. Experimental setup for the Acfer 094 hypervelocity dust shots at the University of Kent. The target material (arrow) is a 1 cm × 1 cm square of *Stardust* flight spare Al 1100 foil.
(A color version of this figure is available in the online journal.)

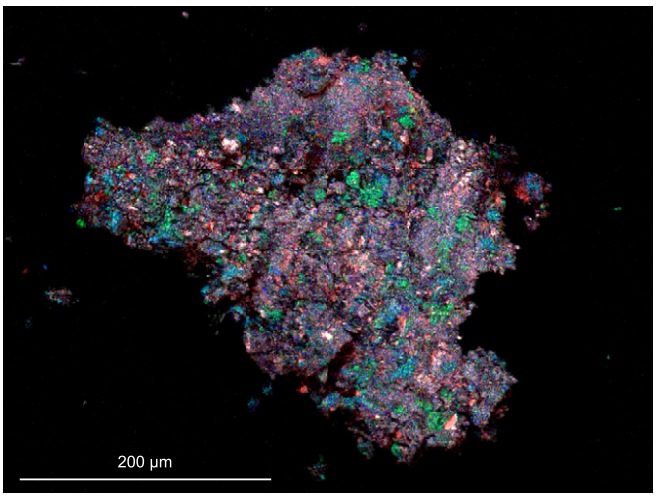

Figure 2. Backscattered electron image of Acfer 094 projectile material with false color overlays of EDX elemental maps, showing that the aggregate powder is well mixed (green = Mg; blue = Si; white = S; yellow = Ca; red = Fe).
(A color version of this figure is available in the online journal.)

two-stage light gas gun at the University of Kent (see Burchell et al. 1999 for details of this method), at impact speeds (~6 km s^{-1}) similar to the nominal *Stardust* encounter speed at comet 81P/Wild 2. The procedures were similar to those originally established for *Stardust* foil calibration shots (e.g., Kearsley et al. 2006). Because of concerns after these two test shots that some fine-grained material might have been left behind in the mortar, a third sample (labeled 3a; Table 1) was prepared by more prolonged grinding to ensure that all of the sample was reduced to very fine grained and well-mixed material (this sample was not sieved). This was followed by impregnation with acrylate aerosol adhesive spray (Winsor and Newton Artists' Fixative Spray), after which the aggregate material was scraped from the mortar for use as projectiles. This procedure ensured that no fine-grained material was left in the mortar and provided aggregates of hundreds to thousands of sub-grains (Figure 2), that were likely more representative of the bulk Acfer 094 sample than the first two test shots. The shots produced heavily cratered target foils, with individual craters between <1 μm and nearly 200 μm in diameter, whose morphologies are virtually indistinguishable from *Stardust* craters (Figure 3).

2.3. NanoSIMS Measurements

Secondary electron images of the foils were obtained at a resolution of ~200 nm/pixel and the images were manually searched for impact craters, as well as assembled into mosaics for sample navigation. Selected areas of some foils were imaged at higher magnifications, allowing the identification of craters down to ~250 nm in diameter.

Raster ion imaging of the crater residues was carried out with a 16 kV, ~1 pA Cs^+ primary ion beam (~100 nm diameter). Secondary ions of C ($^{12}C^-$, $^{13}C^-$) and O ($^{16}O^-$, $^{17}O^-$, $^{18}O^-$) were collected in multi-collection mode, along with secondary

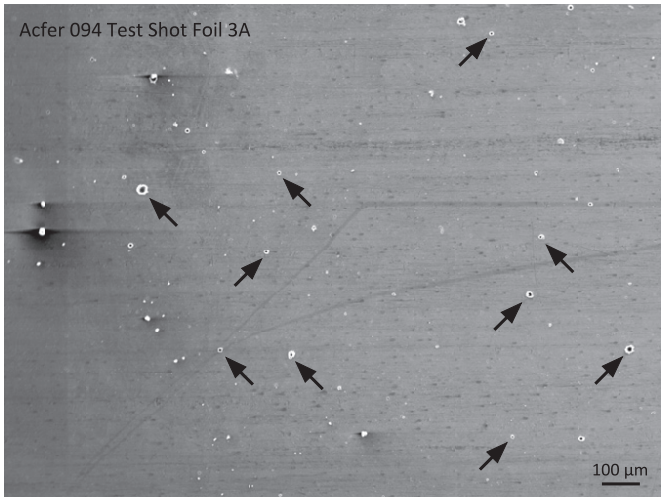

Figure 3. Secondary electron image of Acfer 094 test shot foil 3a showing representative craters.

electrons, at a mass resolution sufficient to separate $^{17}O^-$ from $^{16}O^1H^-$. Imaged areas (256^2 or 512^2 pixels) ranged in size from $3 \times 3\,\mu m^2$ to $40 \times 40\,\mu m^2$, depending on the sizes of the craters (or sections of craters) analyzed, with acquisition of 5–40 layers for each measurement. Data processing for the identification of isotopic anomalies followed routine procedures (e.g., Floss & Stadermann 2009), with normalization to the average composition of residue within the field of view of each measurement, assuming normal bulk isotopic compositions. Because of morphological variations within and among different craters, with residue present on the rims, deep bottoms and steep side walls of the craters, measurements on these samples are more difficult than our usual semi-automated searches of primitive meteorites (e.g., Floss & Stadermann 2009), and manual re-tuning of the secondary ion extraction was typically required both for individual craters and for different areas within larger craters. Consequently, in addition to precluding the use of external standards, because of instrumental fractionation due to sample height variations (Stadermann et al. 2008), it takes significantly longer to acquire a given cumulative search area size for the crater studies. The total surface area of residue searched was determined from the combined C and O ion signals, as well as the SE images from each measurement. Oxygen from the oxide layer on the surface of the Al foil is rapidly sputtered away in the first layers and is, therefore, readily distinguished from the oxygen present in the residue debris itself (e.g., Stadermann et al. 2008).

2.4. Auger Measurements

We used the Auger Nanoprobe to investigate the elemental compositions of some of the presolar grains we found. Auger spectra were obtained with a 10 kV 0.5 nA beam current by rastering over the areas of the grains and collecting multiple spectra which were subsequently added together to constitute a single Auger spectrum for each grain (see Floss & Stadermann 2009 for details). Due to the relatively poor quality of the spectra (e.g., low signal-to-noise), we did not attempt quantification of the data. We also obtained Auger elemental maps, using a 10 kV 10 nA beam current, to investigate the distribution of elements in the areas around the presolar grains.

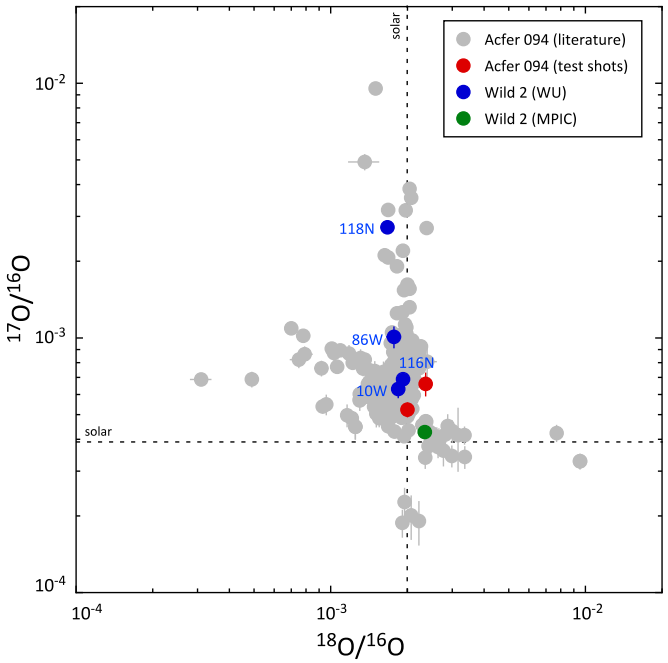

Figure 4. Oxygen three-isotope plot showing O-rich presolar grains from Acfer 094 (literature and test shot crater data) and comet 81P/Wild 2 (McKeegan et al. 2006; Stadermann et al. 2008; Leitner et al. 2010; this study). WU: Washington University in St. Louis; MPIC: Max-Planck-Institut f. Chemie. Acfer 094 literature data are from the Presolar Grain Database (Hynes & Gyngard 2009).

(A color version of this figure is available in the online journal.)

3. RESULTS

3.1. Comet 81P/Wild 2

We identified four O-rich presolar grains in four different craters (Table 2; Figure 4). One of these grains was found during the PE (McKeegan et al. 2006; Stadermann et al. 2008), while the other three were discovered post-PE. All of the grains show enrichments in ^{17}O and solar to sub-solar $^{18}O/^{16}O$ ratios (e.g., Group 1; Nittler et al. 1997). Presolar grain 86W (250 nm diameter) was found within a mass of projectile residue present on the rim of the large (295 μm diameter) penetration crater on foil C2086W (McKeegan et al. 2006; Stadermann et al. 2008). The C and O secondary ion yields suggest that it is an oxide or silicate grain, but FIB extraction and subsequent TEM measurement did not result in successful identification of the grain (Stadermann et al. 2008).

Figure 5 shows the craters and locations of the other three presolar grains identified in our work. Presolar grain 118N is 170 nm in diameter and was found on the rim of a ~70 μm diameter crater on foil C2118N. This is the most ^{17}O-rich grain found to date in comet Wild 2 samples (Table 2). No phase identification was possible because the grain sputtered completely away during the NanoSIMS measurement. Another ^{17}O-rich presolar grain (~235 nm in diameter) was found on the rim of a 28 μm crater from foil C2116N. The Auger spectrum for this grain showed only the presence of Al, O, and C. This could indicate either that the grain is an Al-oxide, or that insufficient material was left after the NanoSIMS measurement to allow detection of other elements; although the NanoSIMS data indicated that the grain was not completely sputtered away, other elements may not have been above the detection limits of the Auger Nanoprobe (~3–5 at.%). Finally, a third, very small

Table 2
Isotopic Compositions of Presolar Grains from Wild 2 and Acfer 094 Test Shots.

Grain	Type	Diameter (nm)	$^{17}O/^{16}O$ ($\times 10^{-4}$)[a]	$^{18}O/^{16}O$ ($\times 10^{-3}$)[a]	$^{12}C/^{13}C$[a]
Wild 2					
86W[b]	Group 1	250	10.1 ± 1.0	1.8 ± 0.1	n.r.
118N	Group 1	170	27 ± 2	1.7 ± 0.1	n.r.
116N	Group 1	235	6.9 ± 0.6	1.9 ± 0.1	n.r.
10W	Group 1	100	6.3 ± 0.5	1.8 ± 0.1	n.r.
Test Shots					
1a SiC	Mainstream	315	n.r.	n.r.	75 ± 3
3a SiC	Mainstream	235	n.r.	n.r.	76 ± 3
2a O-rich	Group 1	295	6.6 ± 0.7	2.4 ± 0.1	
2a O-rich	Group 1	195	5.2 ± 0.4	2.0 ± 0.1	

Notes.
[a] Errors are 1σ.
[b] Data from McKeegan et al. (2006) and Stadermann et al. (2008).

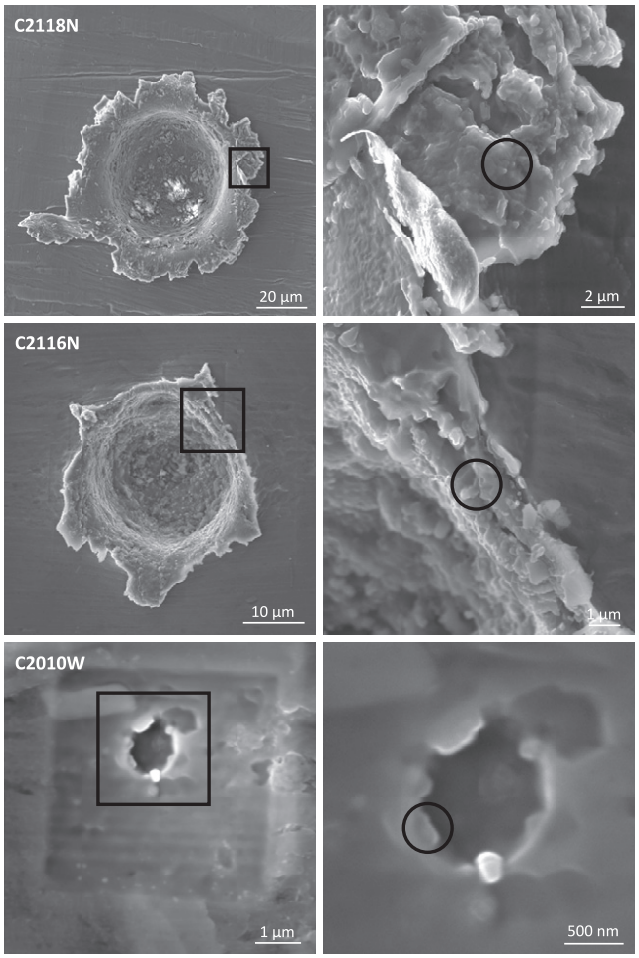

Figure 5. Secondary electron images of comet Wild 2 craters in which presolar grains were observed. The boxes outline the close-up views shown to the right of each crater; the locations of the presolar grains are circled.

(~100 nm diameter) presolar grain was found along the edge of a 1.1 μm crater in foil C2010W. For this grain too, the Auger spectrum is dominated by Al and O; very minor peaks of Mg and Fe are also present, representing less than ~2.5 at.% of these elements (Figure 6). The Auger elemental maps also show the presence of some Mg and Fe, and less Al than in other areas of the image. Silicon does not appear to be present, but this may be due to the low signal-to-noise ratio of the spectrum and the fact that the Si KLL line at 1620 eV is not very strong.

The total surface area of projectile residue that we have measured in *Stardust* craters is ~5000 μm^2. Most of this is material present in and around the three large (28–295 μm) craters in foils C2086W, C2118N, and C2116N; the total area measured on the 20 smaller craters from C2010W is only ~330 μm^2 (Table 1). Based on the sizes of the presolar grains and the total surface area of projectile residue measured, the four grains identified in the *Stardust* craters represent a presolar grain abundance of ~25 ppm (Table 3). The estimates for each foil range between 10 and 45 ppm; the three large craters have abundances of 37 ppm (2086W), 10 ppm (2118N), and 45 ppm (2116N), while the abundance for the 20 craters from 2010W is 24 ppm.

3.2. Acfer 094 Test Shots

In the hypervelocity test shots, we measured a total projectile residue surface area of almost 25,000 μm^2, with approximately 1/3 of the area coming from each of the three foils (Table 1). We examined 88 different craters whose sizes ranged from 1.5 to 90 μm, and identified two O-anomalous and two C-anomalous presolar grains. The O-rich grains, both of which were found on Acfer 094 foil 2a, are ^{17}O-rich Group 1 grains (Figure 4), with diameters of 200–300 nm (Table 2). One of them occurs on the lip of a large (~50 μm diameter) crater, while the other one is on the edge of a 5 μm crater. The C-anomalous grains are both ^{13}C-rich (Table 2); based on their isotopic compositions ($^{12}C/^{13}C = 75 \pm 3$ and 76 ± 3) they are likely to be mainstream SiC grains (e.g., Zinner 2007). One was found on the rim of a 45 μm crater on foil 1a and the other is from a similarly sized crater on foil 3a. Calculation of the abundance of presolar grains, again based on the grain sizes and total surface area of projectile residue measured on these test shots, indicates overall abundances of 4 and 5 ppm (Table 3) for the O-anomalous and SiC grains, respectively. In the discussion below, we compare these results to the expected values and explain how the processes associated with hypervelocity impact at 6 km s^{-1} may bias the observed results.

4. DISCUSSION

4.1. Presolar Grain Abundances in the Stardust Cometary Foil Samples

In the years since their initial discovery (Messenger et al. 2003a; Nguyen & Zinner 2004; Nagashima et al. 2004), presolar silicate grains have been found in abundance in the most

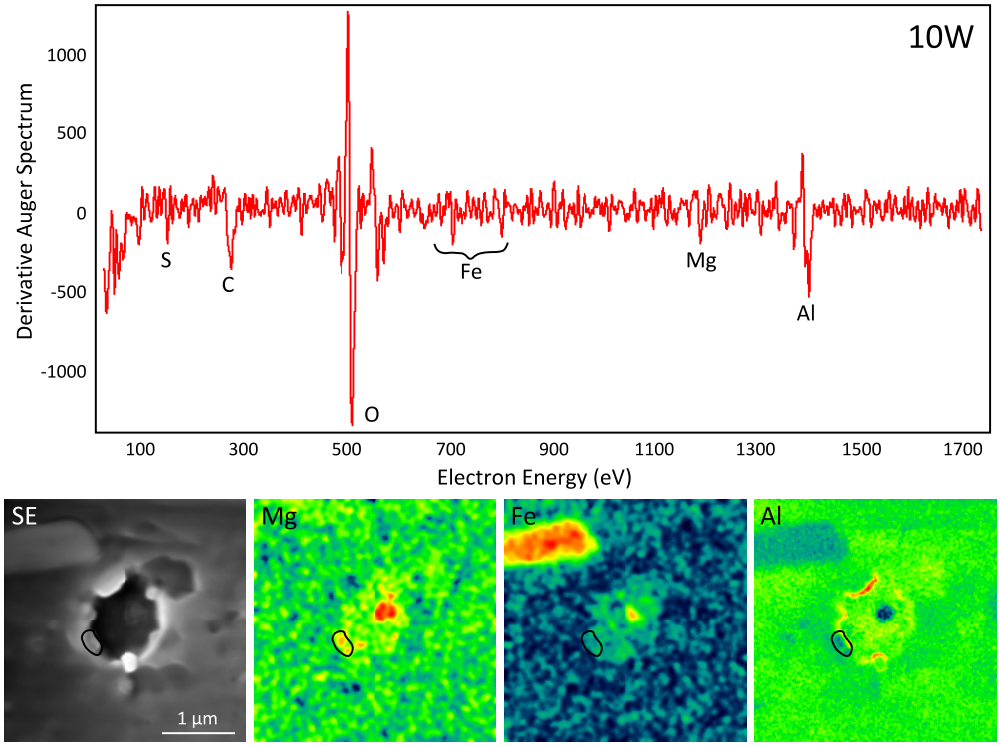

Figure 6. Derivative Auger spectrum (top) and Auger secondary electron and false-color elemental maps (bottom) of the presolar grain-bearing crater from foil C2010W. The presolar grain is outlined.

(A color version of this figure is available in the online journal.)

Table 3
Presolar Grain Abundances in Acfer 094 and Wild 2

Grain	Acfer 094	Wild 2
Residue area searched	24785 μm^2	4995 (+86) μm^2[a]
Presolar grains found		
Silicates and/or oxides	2	4 (+1)[a]
SiC	2	0 (+1)[b]
Nominal (measured) abundance		
Silicates and/or oxides	4 ppm	25 (35) ppm[a]
SiC	5 ppm	15 ppm[b]
Matrix-normalized abundance		
Silicates and/or oxides	145–190 ppm[c]	
SiC	35 ppm[d]	
Bulk abundance[e]		
Silicates and/or oxides	70–95 ppm	~600–830 ppm
SiC	15 ppm	~45 ppm

Notes.
[a] Plus data from Leitner et al. (2012).
[b] Plus SiC identified in aerogel track 141 (Messenger et al. 2009), with the nominal abundance based on the area measured in this work.
[c] data from Mostefaoui & Hoppe (2004), Nguyen et al. (2007), and Vollmer et al. (2009).
[d] Data from Davidson et al. (2009).
[e] Based on a matrix abundance of 51% (Konrad et al. 2010).

primitive solar system materials. Estimates of presolar silicate abundances are typically ~150–200 ppm in primitive carbonaceous chondrites such as Acfer 094, ALHA77307, QUE 99177, and MET 00426 (Nguyen et al. 2007, 2010; Floss & Stadermann 2009; Vollmer et al. 2009) and are even more abundant (⩾375 ppm; Messenger et al. 2003a; Floss et al. 2006; Busemann et al. 2009) in primitive chondritic porous IDPs. Because comet Wild 2 is a Jupiter-family comet that originated in the Kuiper Belt, one of the original expectations from the *Stardust* mission was that the samples returned would, like IDPs, be dominated by primitive materials from the early solar system (including abundant presolar grains), which had remained essentially unaltered over the last 4.5 billion years in the cold environment of the Kuiper Belt. However, results from the PE showed that high-temperature components, like those thought to form in the inner solar system, were abundant in comet Wild 2 (Brownlee et al. 2006; Zolensky et al. 2006), whereas presolar components appeared to be relatively rare (McKeegan et al. 2006; Stadermann et al. 2008). Our present results confirm the scarcity of presolar grains in the impact residues of the *Stardust* craters, with a nominal abundance of ~25 ppm for O-rich silicate/oxide grains. The four grains identified in our work are all Group 1 grains (Nittler et al. 1997), with enrichments in ^{17}O and solar to sub-solar $^{18}O/^{16}O$ ratios; the isotopic compositions of these grains are consistent with origins in low-mass asymptotic giant branch (AGB) stars of close-to-solar metallicity.

A fifth O-rich presolar grain was found by Leitner et al. (2010, 2012) in a 700 nm crater from foil C2037N. This grain is enriched in ^{18}O (Group 4: Figure 4) and probably formed in the ejecta of a type II supernova. Inclusion of this grain and the total residue area measured by Leitner et al. (2012) revises the abundance of O-rich presolar grains from ~25 ppm to ~35 ppm, still an order of magnitude less than the abundances observed in primitive IDPs (Floss et al. 2006), which are generally thought to have a cometary origin. Although no presolar SiC has been found in the crater searches carried out to date, Messenger et al. (2009) did identify a mainstream SiC grain in aerogel track 141 (e.g., Coki). Based on the size of this grain and the area measured

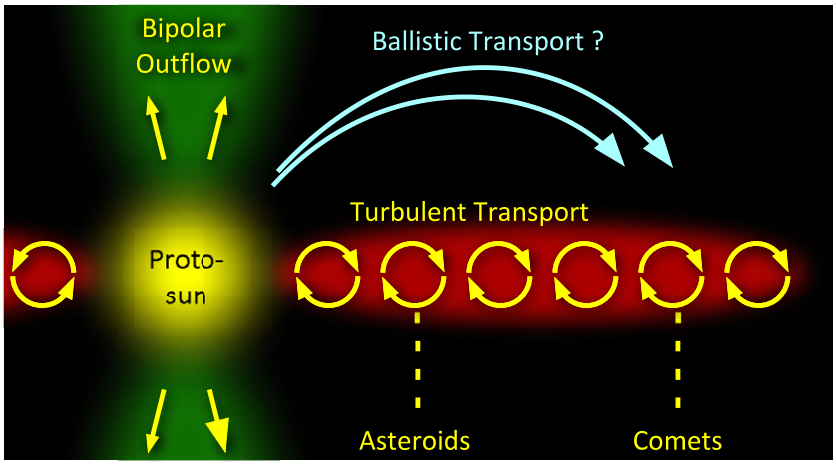

Figure 7. Schematic illustrating possible mechanisms for transport of material from the inner solar nebula to the outer, comet-forming region.
(A color version of this figure is available in the online journal.)

in the foil crater searches, we estimate an SiC abundance of ~15 ppm (Table 3).

Variations in presolar grain abundances from different host materials are typically explained by different degrees of secondary processing, such as thermal metamorphism or aqueous alteration, which can lead to partial or complete loss of the identifying features of presolar materials. For example, Nagashima et al. (2005) carried out an extensive survey of the CM chondrite Murchison and determined a presolar silicate abundance of ~3 ppm, significantly lower than that observed in other primitive chondrites. They attributed this difference to the aqueous alteration experienced by this meteorite. More recently, Floss & Stadermann (2012) argued that thermal processing was responsible for the low abundance (~70 ppm) of presolar silicates in the Adelaide ungrouped carbonaceous chondrite and, moreover, had altered the elemental compositions of those presolar silicates still present. However, as noted above, such parent body processes are not expected to be important on comet Wild 2, which has spent the majority of its life in the outer solar system, and whose mineral components suggest little pervasive parent body processing (Brownlee et al. 2012).

An alternative explanation for the low presolar grain abundances in the *Stardust* samples is dilution with solar system material. The presence of high-temperature phases in these samples (e.g., Brownlee et al. 2006) indicates that there was large-scale mixing in the early solar nebula and the fraction of inner solar system material present in Wild 2 has been estimated to be more than 50% (Westphal et al. 2009). Relative to the high abundance of presolar grains found in primitive IDPs, the material collected from Wild 2 would need to be diluted by ~90%–95% presolar-grain-free matter to account for the observed abundances. Such extensive mixing would require a very efficient transport mechanism. Modeling by Ciesla (2007) has shown that turbulent transport in the midplane of the nebula will move significant amounts of inner solar system material to the outer nebula where comets form (Figure 7). Alternatively, ballistic transport above the midplane, such as the X-wind model of Shu et al. (2001), would also allow for the transfer of material from the inner nebula to the comet-forming region. Although the high-temperature components present in Wild 2 clearly attest to the fact that such transport did occur, the very high degree of dilution required to account for the low presolar grain abundances observed suggests that other factors must also have played a role.

4.2. Calibrating Presolar Grain Abundance Determinations in Impact Craters

Our searches for presolar grains in the *Stardust* samples are conceptually similar to presolar grain searches on meteorite thin sections or grain size separates (e.g., Floss & Stadermann 2009; Bose et al. 2010), but the actual implementation is more difficult in the case of the impact craters. Three dominant factors contribute to the uncertainty in determining the presolar grain abundance of Wild 2 samples: (1) the limited statistics available, (2) the difficulty in accurately defining the measured reference area, and (3) the possibility of selective sample destruction during the hypervelocity impacts (Stadermann et al. 2008). We will consider each of these in turn.

Because the impact craters show significant morphological variations, with cometary debris found on the rims, the deep bottom and the steep side walls of the craters, it is not possible to carry out the semi-automated searches that we use for primitive meteorites. Typically, careful retuning of the secondary ion extraction is needed, not just for each individual crater, but also for different areas within the larger craters. Thus, it takes significantly longer to obtain a statistically meaningful search area size in the crater studies. Although we have now searched ~5000 μm^2 of area in the *Stardust* craters, this is still an order of magnitude less than the amount of area that has been searched in meteorites such as Acfer 094 and ALHA77307 (Vollmer et al. 2009; Bose et al. 2010, 2012; Nguyen et al. 2007, 2010). It is, however, comparable (within a factor of two) to the areas searched in the CR3 chondrites QUE 99177 and MET 00426 by Floss & Stadermann (2009) and is significantly higher than the total area that has been examined in IDPs (e.g., Messenger et al. 2003a, 2005; Floss et al. 2006, 2010; Busemann et al. 2009). All of these samples have high presolar grain abundances, indicating that the low abundances determined from the *Stardust* Al foil measurements are statistically significant. Nevertheless, continued isotopic measurements of the residues found in cometary foil impact craters are desirable for improved accuracy.

A second complicating factor is the difficulty in determining the reference area size for the presolar grain abundance calculations. The reason for this is that it is not always possible to unequivocally delineate genuine projectile residue and partially melted target material, particularly when both are heterogeneously mixed on a fine scale. Figure 8 illustrates how the

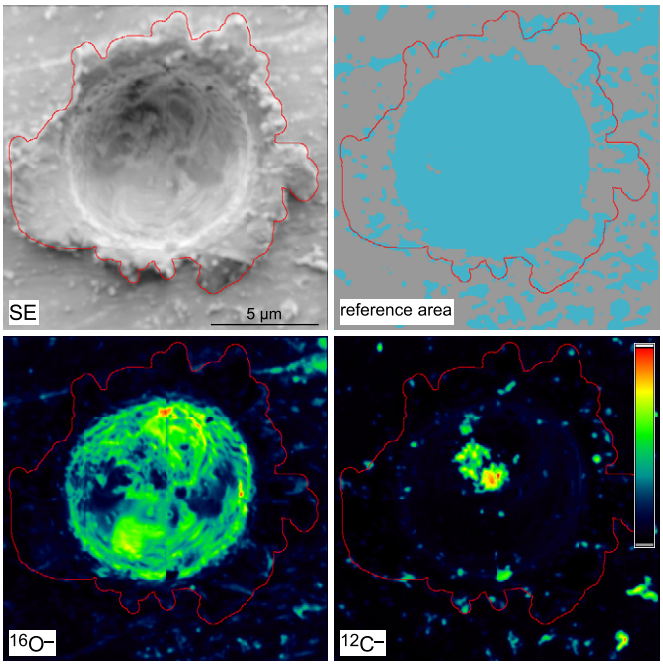

Figure 8. Secondary electron (SE) and false-color secondary ion images of a crater from Acfer 094 test shot foil 2a. The outline shows the region of interest defined from the SE image and the reference area (or fraction of projectile residue) is determined from the $^{12}C^-$ and $^{16}O^-$ ion images, with a threshold applied to exclude those regions with counts too low to obtain statistically meaningful data.

(A color version of this figure is available in the online journal.)

fraction of projectile residue present in the impact craters was determined in this work. The applicable region of interest was selected from the SE image and the reference area (or fraction of projectile residues) was determined from the $^{12}C^-$ and $^{16}O^-$ ion images, with a threshold applied to exclude those regions with counts too low to obtain statistically meaningful isotopic ratios. Although uncertainties remain with this approach (e.g., the presence of residue that is neither C- nor O-rich, or the presence of C- and/or O-bearing contaminants in the Al foil), these factors are not likely to contribute significantly to the overall projectile area determination.

Finally, hypervelocity impacts incur mechanical stress and elevated temperatures, which can result in alteration and/or destruction of material from the original projectile. This raises the question of whether the abundance of presolar grains in the crater residues is the same as that in the original comet dust. Figure 9 shows several scenarios of what may occur to a projectile during hypervelocity impact. One possibility is that only a fraction of the projectile survives, but the relative proportions of the different components remains the same. In this scenario, there is no preferential loss of presolar grains relative to other components, and the presolar grain abundances in the residues will be representative of the original projectile. Another possibility is that, upon impact, the grains in the projectile will break up into smaller fragments. If the presolar grains are smaller, their isotopic signatures are more likely to be diluted with surrounding isotopically normal material, resulting in a decreased detection efficiency during the measurements (e.g., Nguyen et al. 2007) and, consequently, lower apparent abundances. A final possibility is that the heating which takes place upon impact creates a melt mixture, and the isotopic anomalies carried by the presolar grains become diluted in the melt. In this scenario, the measured presolar grain abundances will also be lower than the actual abundances.

We tested these possibilities by carrying out hypervelocity impact shots using powdered samples of the Acfer 094 carbonaceous chondrite, for which presolar grain abundances are well established (e.g., Nguyen et al. 2007; Vollmer et al. 2009). By searching the impact residues of these test shots for presolar grains under the same conditions used for the *Stardust* searches, we are able to determine relative grain-type specific survival probabilities, which can then be used to calibrate the presolar grain abundances in comet 81P/Wild 2. Moreover, using these data for calibration purposes allows us to compensate for any systematic errors in the determination of reference area size, including possible operator bias, as such errors should be very similar between *Stardust* and our experiment and will effectively cancel out.

Acfer 094 has been the object of several NanoSIMS ion imaging studies to search for O-rich presolar grains. These studies indicate abundances of presolar silicate and oxide grains ranging from 145 to 190 ppm (Mostefaoui & Hoppe 2004; Nguyen et al. 2007; Vollmer et al. 2009). The abundance of presolar SiC has been estimated at 35 ppm (Davidson et al. 2009). In both cases, the abundances are matrix-normalized. Assuming a matrix fraction of 51 vol.% (Konrad et al. 2010) gives bulk abundances of 70–95 ppm for silicates and oxides and ∼15 ppm for SiC in this meteorite. Our imaging searches on the Acfer 094 test shot foils identified two O-rich presolar grains and two presolar SiC, resulting in measured abundances of 4 and 5 ppm, respectively (Table 3). Given the bulk abundances noted above, the number of grains we would expect to find in the area we have measured on these foils (∼25,000 μm^2) is on the order of 25–75 for silicates and oxides, and 5–10 for SiC, assuming grain sizes between 200 nm and 300 nm. This clearly demonstrates the destruction or re-equilibration of a large fraction of the presolar grains as a result of the hypervelocity impacts into Al foil, with a loss of more than 90% of the presolar silicates and oxides in Acfer 094. The fraction of SiC lost is lower, indicating a higher resistance to destruction.

Many of the presolar grains are undoubtedly lost from the crater during the impact, but this alone probably does not result in preferential loss, as much of the other material in the projectiles is also ejected or vaporized. As discussed above, preferential loss of recognizable presolar grains is likely to be due to dilution of the anomalous isotopic signatures carried by the grains (e.g., Figure 9). The ^{18}O enrichment of the presolar grain found by Leitner et al. (2010) in a small Wild 2 crater is distributed over much of the crater area, evidence that the projectile experienced melting upon impact and the isotopic signature of the presolar grain was diluted in the melt mixture (Scenario 3 in Figure 9). However, the isotopic signatures of the other four O-rich presolar grains from Wild 2 do not show this distribution over larger areas in the NanoSIMS isotope ratio plots and, thus, do not appear to have been melted. The presolar O-rich and SiC grains from the Acfer 094 test shots also do not show evidence of melting. Hypervelocity impact studies using *Stardust* analog materials have shown that, although crystalline components can be preserved, impact-generated melts are common, particularly in impacts of aggregate materials. Wozniakiewicz et al. (2012a) carried out TEM analysis of an impact crater created by a monodisperse aggregate projectile consisting of a mixture of fine olivine, diopside, and pyrrhotite powders. They found that the residue consisted predominantly of small Fe-rich crystalline beads within a compositionally variable alumino-silicate glass

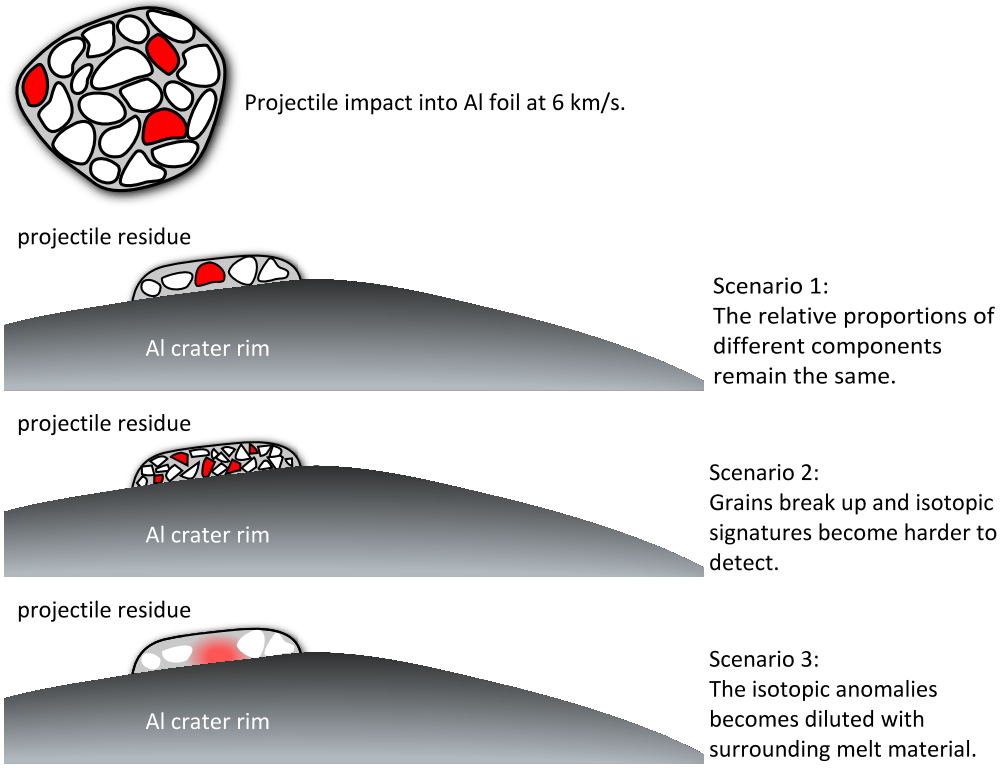

Figure 9. Schematic illustrating possible outcomes upon projectile impact into Al foil under *Stardust*-like conditions.
(A color version of this figure is available in the online journal.)

that was vesiculated in some locations. No surviving crystalline minerals were observed in the residue of this impact crater, although crystalline components do survive in residues from most larger ($>10\,\mu$m) single grain impacts (Wozniakiewicz et al. 2012a, 2012b). However, TEM analyses of craters from the *Stardust* Al foils themselves do show evidence of crystalline materials representing surviving impactor material in craters with mixed (sulfide and silicate) compositions (Leroux et al. 2008). Wozniakiewicz et al. (2012a) noted that their monodisperse aggregate may not be representative of typical *Stardust* impactors, which are likely to be more variable in size, possibly allowing larger grains to escape complete melting. Moreover, the experimental work shows that projectile behavior during impact is complex, with subgrain interactions dependent on many factors, including grain size, impactor internal structure, and target properties (Wozniakiewicz et al. 2012a). Although beyond the scope of this paper, TEM analysis of residues containing presolar grains (from both the *Stardust* cometary foils and the Acfer 094 test shot foils) will be important in order to gain a detailed understanding of the conditions leading to survival of these grains during the impact process.

4.3. Presolar Grain Abundances in Comet 81P/Wild 2

As discussed above, our results from the Acfer 094 test shots indicate the loss of a significant fraction of the presolar grains originally present in this meteorite. If we assume a similar loss rate for the *Stardust* cometary samples, we can calculate their original pre-impact presolar grain abundances. For the O-rich presolar grains, the measured abundance of 35 ppm in the cometary foils suggests original abundances between 600 and 830 ppm, based on the 70–95 ppm range of O-rich presolar grains in bulk Acfer 094 (Table 3). Estimates of the fraction of matrix material in Acfer 094 range between 45 vol.% (Wasson 2008) and 62 vol.% (Newton et al. 1995); the estimate of Konrad et al. (2010) falls in the middle of this range and, therefore, provides an intermediate range of values for the abundance of presolar grains in the *Stardust* samples. The original abundance of SiC can be similarly calculated and is estimated to be ~45 ppm.

There are several key uncertainties with respect to these estimates for the abundances of presolar grains in the *Stardust* samples. First is the question of whether the assumption of similar presolar grain-loss rates between the Acfer 094 test shots and the *Stardust* samples is valid. In terms of impact parameters, the two sets are largely equivalent; the hypervelocity impact experiments were conducted under conditions similar to those experienced by the actual *Stardust* samples and the same Al 1100 foil was used as the target material. Similarly, the NanoSIMS measurements and data processing routines were identical for both sample sets. Differences in the impactor compositions could, however, affect the impact behavior of the projectiles and, consequently, the survivability of presolar grains. Comets consist of mixtures of ice and dust preserved from the early formation of the solar system, and the presence of abundant ice in the projectiles would likely lead to impact behavior that differed significantly from that of ice-free projectiles, like the Acfer 094 test shots. However, Brownlee et al. (2006) noted that the *Stardust* cometary collection is likely to be dominated by the non-volatile component of Wild 2, as the material largely originated from jets driven by the sublimation of water ice and most ice components were probably volatilized during transit from the comet to the spacecraft collector. This non-volatile component of Wild 2, consisting of mixtures of fine-grained nebular materials and fragments from the disruption of larger particles (e.g., Davis & Farinella 1997), should be largely similar

to the type of material comprising Acfer 094 and, thus, we would not expect large differences in the impact behavior of these two types of projectiles.

Another uncertainty concerns the question of how representative the *Stardust* samples are of the comet itself. Throughout its 4.5 billion year history, the surface of comet Wild 2 will have interacted with other solar system materials present in the regions where it has resided, which could have led to alteration of its surface material or contamination with more recent solar system materials. This concern also appears unlikely, as cometary activity since Wild 2 entered the inner solar system has caused it to lose its original surface through the sublimation of water ice, leading to loss of gas, rocks, and dust at rates of tons per second (Brownlee et al. 2006). Moreover, the particles sampled by the *Stardust* collectors originated from numerous collimated jets of solid particles ejected from the interior of the comet (Sekanina et al. 2004) and, therefore, should be representative of the material that accreted (along with ices) to form the comet 4.5 billion years ago (Brownlee et al. 2006). Thus, we are confident that the abundances estimated here are a reasonable approximation of the original presolar grain abundances present in comet 81P/Wild 2 at the time of its formation.

Our range of abundances calculated for presolar silicates and oxides in Wild 2 (600–830 ppm) is essentially in agreement with the 1100 ppm determined by Leitner et al. (2012), given the uncertainty associated with abundance determinations based on a single grain (e.g., Gehrels 1986). These abundances are also consistent with those determined for IDPs, which range from ∼375 ppm for a suite of isotopically primitive IDPs (Floss et al. 2006) to as high as 15,000 ppm for a single IDP from the Grigg–Skjellerup targeted collector L2054 (Busemann et al. 2009). In contrast, the most primitive meteorites have matrix-normalized abundances of presolar silicates and oxides in the range of 150–200 ppm, significantly lower than the estimates for Wild 2; bulk abundances will be lower by roughly a factor of two, depending on the fraction of matrix in the meteorite. For presolar SiC, we obtain a calibrated abundance for Wild 2 of ∼45 ppm, which is broadly consistent with the range of abundances determined for a variety of meteorites by NanoSIMS ion imaging of IOM residues (10–55 ppm; Davidson et al. 2009). The consistency of the SiC abundances between Wild 2 and primitive meteorites, in contrast to the difference observed for O-rich presolar grains reflects, as we noted above, the higher resistivity of SiC to destruction, compared to presolar silicates and oxides. Interestingly enough, only one presolar SiC has been identified in IDPs to date (Stadermann et al. 2006). These authors report an abundance of 60 ppm for SiC in just that IDP, but note that if all IDPs are considered, the abundance is significantly lower.

Primitive IDPs have long been associated with comets, because their high abundances of presolar silicates and the presence of pristine insoluble organic matter with abundant H, C, and N isotopic anomalies (e.g., Messenger et al. 2003a, 2003b; Floss et al. 2004, 2006, 2010; Busemann et al. 2009) suggest formation in the cold outer regions of the solar nebula. Moreover, Brownlee et al. (1995) showed that stepped He release profiles suggested cometary origins for a group of chondritic porous IDPs. The initial findings of low presolar grain abundances (McKeegan et al. 2006; Stadermann et al. 2008) and the presence of abundant refractory materials from the inner solar system (Brownlee et al. 2006; Zolensky et al. 2006) in the *Stardust* samples revised our understanding of the constituents of comets, and raised questions about the relationships between IDPs and comets.

Our work clarifies one aspect of these early findings and shows that comet Wild 2, in fact, does contain more presolar grains than measurements on the *Stardust* samples suggest. Comet Wild 2 and primitive IDPs have similar presolar silicate abundances, which are significantly higher than even the most primitive meteorites. Both also consist of highly unequilibrated assemblages of solar and presolar materials, consistent with accretion in the outer cold regions of the solar nebula. These similarities support arguments for the cometary origin of primitive IDPs. In contrast, the lower presolar silicate abundances observed in even the most primitive meteorites indicates that the accretion processes they experienced, likely in warmer regions of the solar nebula, were sufficient to destroy a substantial fraction of these grains.

This work was supported by NASA grant NNX10AH07G (PI: C. Floss). Light gas gun work at the University of Kent was supported by a grant from STFC. The authors appreciate the careful review of an anonymous reviewer.

REFERENCES

A'Hearn, M. F. 2006, Sci, 314, 1708
Amari, S., Anders, E., Virag, A., & Zinner, E. 1990, Natur, 345, 238
Bernatowicz, T. J., Croat, T. K., & Daulton, T. L. 2006, in Meteorites and the Early Solar System II, ed. D. S. Lauretta et al. (Tucson, AZ: Univ. Arizona Press), 109
Bland, P. A., Stadermann, F. J., Floss, C., et al. 2007, M&PS, 42, 1417
Bose, M., Floss, C., & Stadermann, F. J. 2010, ApJ, 714, 1624
Bose, M., Floss, C., Stadermann, F. J., Stroud, R. M., & Speck, A. K. 2012, GeCoA, 93, 77
Brownlee, D. E., Hörz, F., Newburn, R. L., et al. 2004, Sci, 304, 1764
Brownlee, D. E., Joswiak, D. J., Schlutter, D. J., et al. 1995, in Lunar Planet. Sci., Vol. 26, ed. S. J. Mackwell (League City, TX: LPI), 183
Brownlee, D. E., Joswiak, D., & Matrajt, G. 2012, M&PS, 47, 453
Brownlee, D. E., Joswiak, D., Matrajt, G., Messenger, S., & Ito, M. 2009, in Lunar Planet. Sci., Vol. 40, ed. S. J. Mackwell (League City, TX: LPI), abstract 2195
Brownlee, D. E., Tsou, P., Aléon, J., et al. 2006, Sci, 314, 1711
Brownlee, D. E., Tsou, P., Anderson, J. D., et al. 2003, JGR, 108, 1
Burchell, M. J., Cole, M. J., McDonnell, J. A. M., & Zarnecki, J. C. 1999, MeSCT, 10, 41
Burchell, M. J., Fairey, S. A. J., Wozniakiewicz, P., et al. 2008, M&PS, 43, 23
Burchell, M. J., Graham, G., & Kearsley, A. 2006, AREPS, 34, 385
Burchell, M. J., & Kearsley, A. T. 2009, P&SS, 57, 1146
Busemann, H., Nguyen, A. N., Cody, G. D., et al. 2009, E&PSL, 288, 44
Ciesla, F. J. 2007, Sci, 318, 613
Davidson, J., Busemann, H., Alexander, C. M. O'D., et al. 2009, in Lunar Planet. Sci., Vol. 40, ed. S. J. Mackwell (League City, TX: LPI), abstract 1853
Davis, D. R., & Farinella, P. 1997, Icar, 125, 50
Farnham, T. L., Samarasinha, N. H., & Mueller, B. E. A. 2010, IAU Circ., 9138
Farnham, T. L., & Schleicher, D. G. 2005, Icar, 173, 533
Floss, C., & Stadermann, F. J. 2009, GeCoA, 73, 2415
Floss, C., & Stadermann, F. J. 2012, M&PS, 47, 992
Floss, C., Stadermann, F. J., Bradley, J. P., et al. 2004, Sci, 303, 1355
Floss, C., Stadermann, F. J., Bradley, J. P., et al. 2006, GeCoA, 70, 2371
Floss, C., Stadermann, F. J., Mertz, A. F., & Bernatowicz, T. 2010, M&PS, 45, 1889
Gehrels, N. 1986, ApJ, 303, 336
Gyngard, F., Amari, S., Zinner, E., & Ott, U. 2009, ApJ, 694, 359
Hörz, F., Bastien, R., Borg, J., et al. 2006, Sci, 314, 1716
Huss, G. R. 1990, Natur, 347, 159
Huss, G. R. 1997, in Astrophysical Implications of the Laboratory Study of Presolar Materials, ed. T. J. Bernatowicz & E. Zinner (Woodbury, NY: AIP), 721
Huss, G. R. 2004, AMR, 17, 132
Huss, G. R., & Lewis, R. S. 1995, GeCoA, 59, 115
Huss, G. R., Meshik, A. P., Smith, J. B., & Hohenberg, C. M. 2003, GeCoA, 67, 4823
Huss, G. R., Rubin, A. E., & Grossman, J. N. 2006, in Meteorites and the Early Solar System II, ed. D. S. Lauretta et al. (Tucson, AZ: Univ. Arizona Press), 567

Hynes, K. M., & Gyngard, F. 2009, in Lunar Planet. Sci., Vol. 40, ed. S. J. Mackwell (League City, TX: LPI), abstract 1198
Kearsley, A. T., Borg, J., Graham, G. A., et al. 2008, M&PS, 43, 1
Kearsley, A. T., Burchell, M. J., Hörz, F., Cole, M. J., & Schwandt, C. S. 2006, M&PS, 41, 167
Kearsley, A. T., Burchell, M. J., Price, M. C., et al. 2012, M&PS, 47, 737
Konrad, K., Ebel, D. S., & McKnight, S. V. 2010, in Lunar Planet. Sci., Vol. 41, ed. S. J. Mackwell (League City, TX: LPI), abstract 1447
Królikowska, M., & Szutowicz, S. 2006, A&A, 448, 401
Leitner, J., Hoppe, P., & Heck, P. R. 2010, in Lunar Planet. Sci., Vol. 41, ed. S. J. Mackwell (League City, TX: LPI), abstract 1607
Leitner, J., Heck, P. R., Hoppe, P., & Huth, J. 2012, in Lunar Planet. Sci., Vol. 43, ed. S. J. Mackwell (League City, TX: LPI), abstract 1839
Leroux, H. 2012, M&PS, 47, 613
Leroux, H., Stroud, R. M., Dai, Z. R., et al. 2008, M&PS, 43, 143
Lewis, R. S., Tang, M., Wacker, J. F., Anders, E., & Steel, E. 1987, Natur, 326, 160
McKeegan, K. D., Aléon, J., Bradley, J., et al. 2006, Sci, 314, 1724
Messenger, S., Joswiak, D., Ito, M., Matrajt, G., & Brownlee, D. E. 2009, in Lunar Planet. Sci., Vol. 40, ed. S. J. Mackwell (League City, TX: LPI), abstract 1790
Messenger, S., Keller, L. P., & Lauretta, D. S. 2005, Sci, 309, 737
Messenger, S., Keller, L. P., Stadermann, F. J., Walker, R. M., & Zinner, E. 2003a, Sci, 300, 105
Messenger, S., Stadermann, F. J., Floss, C., Nittler, L. R., & Mukhopadhyay, S. 2003b, SSRv, 106, 155
Meyer, B. S., & Zinner, E. 2006, in Meteorites and the Early Solar System II, ed. D. S. Lauretta et al. (Tucson, AZ: Univ. Arizona Press), 69
Mostefaoui, S., & Hoppe, P. 2004, ApJL, 613, 149
Nagashima, K., Krot, A. N., & Yurimoto, H. 2004, Natur, 428, 921
Nagashima, K., Sakamoto, N., & Yurimoto, H. 2005, in Lunar Planet. Sci., Vol. 36, ed. S. J. Mackwell (League City, TX: LPI), abstract 1671
Newton, J., Bischoff, A., Arden, J. W., et al. 1995, Metic, 30, 47
Nguyen, A. N., Nittler, L. R., Stadermann, F. J., Stroud, R. M., & Alexander, C. M. O'D. 2010, ApJ, 719, 166
Nguyen, A. N., Stadermann, F. J., Zinner, E., et al. 2007, ApJ, 656, 1223
Nguyen, A. N., & Zinner, E. 2004, Sci, 303, 1496
Nittler, L. R. 2005, ApJ, 618, 281
Nittler, L. R., Alexander, C. M. O'D., Gao, X., Walker, R. M., & Zinner, E. 1997, ApJ, 483, 475
Price, M. C., Kearsley, A. T., Burchell, M. J., et al. 2010, M&PS, 45, 1409
Sekanina, Z., Brownlee, D. E., Economou, T. E., Tuzzolino, A. J., & Green, S. F. 2004, Sci, 304, 1769
Shu, F. H., Shang, H., Gounelle, M., Glassgold, A. E., & Lee, T. 2001, ApJ, 548, 1029
Stadermann, F. J., & Floss, C. 2008, in Lunar Planet. Sci., Vol. 39, ed. S. J. Mackwell (League City, TX: LPI), abstract 1889
Stadermann, F. J., Floss, C., Gavinsky, A., Kearsley, A. T., & Burchell, M. J. 2009a, in Lunar Planet. Sci., Vol. 40, ed. S. J. Mackwell (League City, TX: LPI), abstract 1188
Stadermann, F. J., Floss, C., Kearsley, A. T., & Burchell, M. J. 2009b, GeCoA, 73, A1262
Stadermann, F. J., Floss, C., & Wopenka, B. 2006, GeCoA, 70, 6168
Stadermann, F. J., Hoppe, P., Floss, C., et al. 2008, M&PS, 43, 299
Tang, M., & Anders, E. 1988, GeCoA, 52, 1235
Trigo-Rodríguez, J. M., & Blum, J. 2009, PASA, 26, 289
Trigo-Rodríguez, J. M., Domínguez, G., Burchell, M. J., Hörz, F., & Lorca, J. 2008, M&PS, 43, 75
Tsou, P., Brownlee, D. E., Sandford, S. A., Hörz, F., & Zolensky, M. E. 2003, JGR, 108, 8113
Vollmer, C., Hoppe, P., Stadermann, F. J., Floss, C., & Brenker, F. E. 2009, GeCoA, 73, 7127
Wasson, J. T. 2008, Icar, 195, 895
Westphal, A. J., Fakra, S., Gainsforth, Z., et al. 2009, in Lunar Planet. Sci., Vol. 40, ed. S. J. Mackwell (League City, TX: LPI), abstract 1819
Wild, P. 1978, IAU Circ., 3166
Wozniakiewicz, P. J., Ishii, H. A., Kearsley, A. T., et al. 2012a, M&PS, 47, 708
Wozniakiewicz, P. J., Kearsley, A. T., Ishii, H. A., et al. 2012b, M&PS, 47, 660
Yada, T., Floss, C., Stadermann, F. J., et al. 2008, M&PS, 43, 1287
Zinner, E. 2007, in Treatise on Geochemistry, ed. H. D. Holland et al. (Oxford: Elsevier)
Zolensky, M. E., Zega, T. J., Yano, H., et al. 2006, Sci, 314, 1735